Optimization of Pin-Fin Heat Sinks in Bypass Flow Using Entropy Generation Minimization Method

W. A. Khan
Associate Professor
Department of Engineering Sciences,
National University of Sciences and Technology,
PN Engineering College, PNS Jauhar,
Karachi, Sindh 75350, Pakistan

J. R. Culham
Associate Professor and Director
Microelectronic Heat Transfer Laboratory,
Department of Mechanical Engineering,
University of Waterloo,
Waterloo, ON, N2L 3G1, Canada

M. M. Yovanovich
Distinguished Professor Emeritus
Department of Mechanical Engineering,
University of Waterloo,
Waterloo, ON, N2L 3G1, Canada

An entropy generation minimization method is applied to study the thermodynamic losses caused by heat transfer and pressure drop for the fluid in a cylindrical pin-fin heat sink and bypass flow regions. A general expression for the entropy generation rate is obtained by considering control volumes around the heat sink and bypass regions. The conservation equations for mass and energy with the entropy balance are applied in both regions. Inside the heat sink, analytical/empirical correlations are used for heat transfer coefficients and friction factors, where the reference velocity used in the Reynolds number and the pressure drop is based on the minimum free area available for the fluid flow. In bypass regions theoretical models, based on laws of conservation of mass, momentum, and energy, are used to predict flow velocity and pressure drop. Both in-line and staggered arrangements are studied and their relative performance is compared to the same thermal and hydraulic conditions. A parametric study is also performed to show the effects of bypass on the overall performance of heat sinks. [DOI: 10.1115/1.2965209]

1 Introduction

Pin-fin heat sinks provide a large surface area for the dissipation of heat and effectively reduce the thermal resistance of the package at the cost of a higher pumping power. They often take less space and contribute less to the weight and cost of the product. For these reasons, they are widely used in applications where heat loads are substantial and/or where space is limited. They are also found to be useful in situations where the direction of the approaching flow is unknown or may change. They are usually mounted on circuit boards where significant clearances are available on the sides and at the top. Due to a higher resistance for the flow through the heat sink, the approaching cooling fluid takes a detour around the heat sink, which always results in a better hydraulic performance with lesser thermal performance.

Many researchers [1–12] have conducted experiments to study the effects of side/top bypass clearance ratios on the heat transfer and pressure drop in pin-fin heat sinks. Bejan [13–17] demonstrated the use of entropy generation minimization for optimization in different applications. Culham and Muzychka [18] and Khan et al. [19–22] extended that use in optimizing fully shrouded heat sinks.

Following Kern and Kraus [23], Sonn and Bar-Cohen [24] and Iyengar and Bar-Cohen [25,26] performed a least-material optimization of cylindrical pin-fin, plate-fin, and triangular-fin array geometries by extending the use of the least-material single fin analysis to multiple fin arrays. Bar-Cohen and Jelinek [27] developed guidelines and design equations for optimum plate-fin arrays.

It is obvious from the literature survey that all optimization studies, related to cylindrical pin-fin heat sinks, are limited to the optimization of fully shrouded heat sinks. The authors could not find any study related to the optimization of pin-fin heat sinks in the bypass flow. In this study, all relevant design parameters for pin-fin heat sinks, including clearance ratios, geometric parameters, and flow conditions, are optimized simultaneously by minimizing the dimensionless entropy generation rate N_s subject to manufacturing and design constraints.

Contributed by the Electrical and Electronic Packaging Division of ASME for publication in the Journal of Electronic Packaging. Manuscript received May 18, 2007; final manuscript received December 1, 2007; published online August 1, 2008. Assoc. Editor: Koneru Ramakrishna. Paper presented at the 2007 ASME-JSME Thermal Engineering Conference and Summer Heat Transfer Conference (HT2007), Vancouver, British Columbia, Canada, July 8–12, 2007.

2 Analysis

The front, side, and top views of an in-line pin-fin heat sink are shown in Fig. 1. The dimensions of the baseplate are $W_2 \times L \times t_b$, where W_2 is the width of the heat sink, L is the length measured in the downstream direction, and t_b is the thickness of the baseplate. The dimensions of the duct are $W \times H$, where W is the width and H is the height of the duct. The dimensions of the side bypass are $W_1 \times H_1$, whereas the dimensions of the top bypass are $W \times H_2$. The flow in the side and top bypass regions is assumed as an inviscid flow. The pin-fins can be arranged in an in-line or staggered manner.

Each pin-fin has a diameter D and a height H_{fin}. The dimensionless longitudinal and transverse pitches are $a = S_L/D$ and $b = S_T/D$. The source of heat is applied to the bottom of the heat sink. The flow is assumed to be laminar, steady, and two dimensional. The duct velocity of the fluid is U_d and the ambient temperature is T_a. There is no leakage of fluid from the top or sides. The wall temperature of the pin is $T_w (> T_a)$ and the baseplate temperature is T_b. The side and top clearance ratios are defined as

$$CL_s = \frac{2W_1}{W_2}$$
$$CL_t = \frac{H_2}{H_1} \tag{1}$$

Khan et al. [19] used the law of conservation of mass and energy and obtained the expressions for the average velocities in the side bypass, top bypass, and just in front of heat sink regions.

$$U_1 = \frac{C_2 U_d}{a_1 C_2 + a_2 C_1 + a_f C_1 C_2}$$

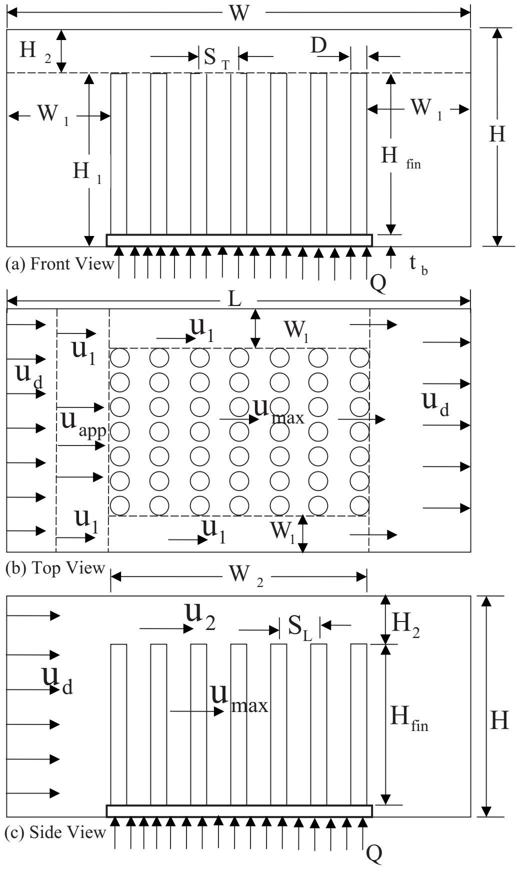

Fig. 1 Front, top, and side views of an in-line pin-fin heat sink in the bypass flow

$$U_2 = \frac{C_1 U_d}{a_1 C_2 + a_2 C_1 + a_f C_1 C_2} \tag{2}$$

$$U_{\text{app}} = \frac{C_1 C_2 U_d}{a_1 C_2 + a_2 C_1 + a_f C_1 C_2}$$

where

$$C_1 = \sqrt{\frac{1+K_1}{1+\sigma_3^2 K_3}} \quad \text{and} \quad C_2 = \sqrt{\frac{1+K_2}{1+\sigma_3^2 K_3}} \tag{3}$$

$$a_1 = \frac{A_1}{A_d}, \quad a_2 = \frac{A_2}{A_d}, \quad a_f = \frac{A_f}{A_d} \tag{4}$$

with

$$K_1 = f_1 \frac{L}{Dh_1}, \quad K_2 = f_2 \frac{L}{Dh_2}, \quad K_3 = f_3(k_c + k_e + f_3 N_L) \tag{5}$$

3 Model Development

In the heat sink region, the entropy generation associated with heat transfer and frictional effects serves as a direct measure of the ability to transfer heat to the surrounding cooling medium. In the bypass regions, entropy generation is associated with the fluid flow only. A model that establishes a relationship between the total entropy generation rate and heat sink design parameters can be optimized in such a manner that all relevant design conditions combine to produce the best possible heat sink for the given constraints. The total entropy generation rate can be written as

$$\dot{S}_{\text{gen}} = \dot{S}_{\text{gen,hs}} + \dot{S}_{\text{gen,bp}} \tag{6}$$

where the entropy generation rate in the heat sink can be obtained by following Khan [28] and Khan et al. [20–22] and applying the laws of conservation of mass and energy with the entropy balance and can be written as

$$\dot{S}_{\text{gen,hs}} = \left(\frac{Q^2}{T_a T_{\text{bp}}}\right) R_{\text{hs}} + \frac{\dot{m}\Delta P_{\text{hs}}}{\rho T_a} \tag{7}$$

Similarly, the entropy generation rate in the bypass region due to the fluid flow can be written as

$$\dot{S}_{\text{gen,bp}} = \frac{\dot{m}\Delta P_{\text{bp}}}{\rho T_a} \tag{8}$$

where ΔP_{bp} is the total pressure drop in the bypass regions and can be written as

$$\Delta P_{\text{bp}} = 2\Delta P_1 + \Delta P_1 \tag{9}$$

with

$$\begin{aligned} \Delta P_1 &= \left(\tfrac{1}{2}\rho U_1^2\right) f_1 (L/D_{h1}) \\ \Delta P_2 &= \left(\tfrac{1}{2}\rho U_2^2\right) f_2 (L/D_{h2}) \end{aligned} \tag{10}$$

where f_1 and f_2 are the friction factors in the side and top bypass regions and are given by

$$f_1 = \frac{24}{\text{Re}_{Dh_1}} \quad \text{and} \quad f_2 = \frac{24}{\text{Re}_{Dh_2}} \tag{11}$$

This assumes a fully-developed flow between parallel plates. Equation (11) shows that the entropy generation rate in the heat sink depends on the heat sink resistance and the pressure drop across the heat sink, provided that the heat load, mass flow rate, and ambient conditions are specified. The lumped heat sink resistance is given by

$$R_{\text{hs}} = R_m + R_{\text{fins}} \tag{12}$$

where R_m is the bulk material resistance given by

$$R_m = \frac{t_{\text{bp}}}{kA} \tag{13}$$

and R_{fins} is the overall resistance of the fins and the exposed baseplate, which can be written as

$$R_{\text{fins}} = \frac{1}{\dfrac{N}{R_c + R_{\text{fin}}} + \dfrac{1}{R_{\text{bp}}}} \tag{14}$$

where

$$\begin{aligned} R_c &= \frac{1}{h_c A_c} \\ R_{\text{fin}} &= \frac{1}{h_{\text{fin}} A_{\text{fin}} \eta_{\text{fin}}} \\ R_{\text{bp}} &= \frac{1}{h_{\text{bp}} A_{\text{bp}}} \end{aligned} \tag{15}$$

with

$$\begin{aligned} \eta_{\text{fin}} &= \frac{\tanh(mH)}{mH} \\ m &= \sqrt{\frac{4h_{\text{fin}}}{kD}} \end{aligned} \tag{16}$$

Khan [28] developed the following analytical correlation for the dimensionless heat transfer coefficient for the cylindrical fin array:

$$\mathrm{Nu}_{D\mathrm{fin}} = \frac{h_{\mathrm{fin}} D}{k_f} = C_3 \mathrm{Re}_D^{1/2} \mathrm{Pr}^{1/3} \tag{17}$$

where C_3 is a constant, which depends on the longitudinal and transverse pitches, arrangement of the pins, and thermal boundary conditions. For isothermal boundary condition, it is given by

$$C_3 = \begin{cases} [0.2 + \exp(-0.55a)] b^{0.285} a^{0.212} & \text{in-line arrangement} \\ \dfrac{0.61 b^{0.091} a^{0.053}}{[1 - 2\exp(-1.09a)]} & \text{staggered arrangement} \end{cases} \tag{18}$$

The heat transfer coefficient for the baseplate, h_{bp}, can be determined by considering it as a finite plate. Khan [28] developed the following analytical correlation for the dimensionless heat transfer coefficient for a finite plate:

$$\mathrm{Nu}_L = \frac{h_{\mathrm{bp}} L}{k_f} = 0.75 \mathrm{Re}_L^{1/2} \mathrm{Pr}^{1/3} \tag{19}$$

where L is the length of the baseplate in the streamwise direction. The mass flow rate through the pins is given by

$$\dot{m} = \rho U_{\mathrm{app}} N_T b H_{\mathrm{fin}} D \tag{20}$$

The pressure drop associated with the flow across the pin-fins is given by

$$\Delta P_{\mathrm{hs}} = f_3 \frac{\rho U_{\max}^2}{2} N_L \tag{21}$$

where the friction factor f depends on the Reynolds number and the array geometry, and it can be written as

$$f_3 = \begin{cases} K_c[0.233 + 45.78/(b-1)^{1.1} \mathrm{Re}_D] & \text{in-line arrangement} \\ K_c[378.6/b^{13.1/b}]/\mathrm{Re}_D^{0.68/b^{1.29}} & \text{staggered arrangement} \end{cases} \tag{22}$$

where K_c is a correction factor depending on the flow geometry and the arrangement of the pins. It is given by

$$K_c = \begin{cases} 1.009 \left(\dfrac{b-1}{a-1} \right)^{1.09/\mathrm{Re}_D^{0.0553}} & \text{in-line arrangement} \\ 1.175(a/b \mathrm{Re}_D^{0.3124}) + 0.5 \mathrm{Re}_D^{0.0807} & \text{staggered arrangement} \end{cases} \tag{23}$$

All the correlations for friction and correction factors are derived from graphs given by Žukauskas [29]. The velocity $U_{\max}$, in Eq. (21), represents the maximum average velocity seen by the array as the flow accelerates between pins and is given by

$$U_{\max} = \max\left\{ \frac{b}{b-1} U_{\mathrm{app}}, \frac{b}{c-1} U_{\mathrm{app}} \right\} \tag{24}$$

where $c = \sqrt{a^2 + (b/2)^2}$ is the dimensionless diagonal pitch.

The dimensionless entropy generation rate can be written as

$$N_s = \dot{S}_{\mathrm{gen}} / (Q^2 U_{\max} / k_f \nu T_a^2) \tag{25}$$

4 Optimization Procedure

The problem considered in this study is to minimize the dimensionless entropy generation rate, given by Eq. (7), for the optimal overall performance of the tube bank. If $f(\mathbf{x})$ represents the dimensionless entropy generation rate that is to be minimized subject to equality constraints $g_j(x_1, x_2, \ldots, x_n) = 0$ and inequality constraints $l_k(x_1, x_2, \ldots, x_n) \geqslant 0$, then the complete mathematical formulation of the optimization problem may be written in the following form:

$$\text{minimize } f(\mathbf{x}) = N_s(\mathbf{x}) \tag{26}$$

subject to equality constraints

$$g_j(\mathbf{x}) = 0, \quad j = 1, 2, \ldots, m \tag{27}$$

and inequality constraints

$$l_j(\mathbf{x}) \geqslant 0, \quad j = m+1, \ldots, n \tag{28}$$

The objective function can be redefined by using the Lagrangian function as follows:

$$\mathcal{L}(\mathbf{x}, \lambda, \chi) = f(\mathbf{x}) + \sum_{j=1}^{m} \lambda_j g_j(\mathbf{x}) - \sum_{j=m+1}^{n} \chi_j l_j(\mathbf{x}) \tag{29}$$

where λ_j and χ_j are the Lagrange multipliers. The λ_j can be positive or negative but the χ_j must be $\geqslant 0$. The necessary condition for $\mathbf{x}^*$ to be a local minimum of the problem, under consideration, is that the Hessian matrix of $\mathcal{L}$ should be positive semidefinite, i.e.,

$$\mathbf{v}^T \nabla^2 [(\mathbf{x}^*, \lambda^*, \chi^*)] \mathbf{v} \geqslant 0 \tag{30}$$

For a local minimum to be a global minimum, all the eigenvalues of the Hessian matrix should be $\geqslant 0$.

A system of nonlinear equations is obtained, which can be solved using numerical methods such as a multivariable Newton–Raphson method. This method has been described in Ref. [30] and applied by Culham and Muzychka [18] and Khan et al. [22] to study the optimization of plate or pin-fin heat sinks. In this study, the same approach is used to optimize the overall performance of a tube bank in such a manner that all relevant design conditions combine to produce the best possible tube bank for the given constraints. The optimized results are then compared for in-line and staggered arrangements.

A simple procedure was coded in MAPLE 10, a symbolic mathematics software, which solves the system of N nonlinear equations using the multivariable Newton–Raphson method. Given the Lagrangian L, the solution vector $[\mathbf{x}]$, the initial guess $[\mathbf{x}_0]$, and the maximum number of iterations $N_{\max}$, the procedure systematically applies the Newton–Raphson method until the desired convergence criteria and/or the maximum number of iterations is achieved. The method is quite robust provided an adequate initial guess is made.

Table 1 Assumed parameter values used for the optimization of cylindrical pin-fin heat sinks in the bypass flow

Quantity	Parameter values
Footprint (mm^2)	50×50
Source dimensions (mm^2)	50×50
Baseplate thickness (mm)	2
Pin diameter (mm)	4
Overall height of heat sink (mm)	50
Duct flow rate (m^3/s)	0.01
Thermal conductivity of solid (W/m K)	210
Thermal conductivity of fluid (W/m K)	0.026
Thermal contact conductance ($\mathrm{W/m^2\,K}$)	10^4
Density of fluid ($\mathrm{kg/m^3}$)	1.1614
Specific heat of fluid (J/kg K)	1007
Kinematic viscosity ($\mathrm{m^2/s}$)	1.58×10^{-5}
Prandtl number	0.71
Heat load (W)	10
Ambient temperature (°C)	27

5 Results and Discussion

The parameters given in Table 1 are used as the default case to determine the thermal and hydraulic resistances and the entropy generation rate for both in-line and staggered pin-fin heat sinks in the bypass flow. The air properties are evaluated at the ambient temperature.

The effect of the side and top clearance ratios on the thermal resistance and the total pressure drop is shown in Fig. 2. In each

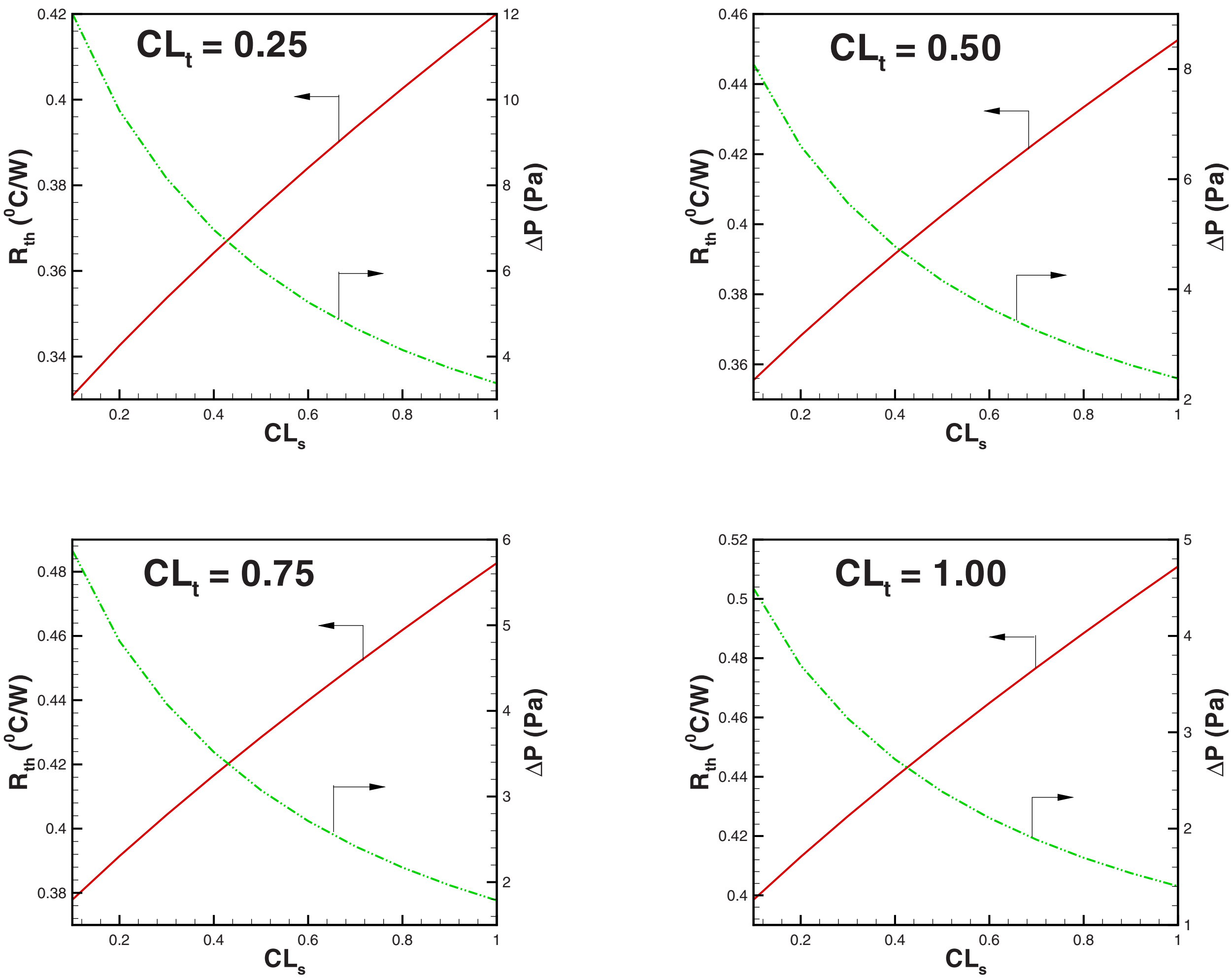

Fig. 2 Thermal resistance and pressure drop in the side and top bypass flows

case, the thermal resistance increases while the pressure drop decreases with the increase in the side and/or top clearance ratios, respectively. It is due to the fact that with the increase in the side or top clearance ratio, the pressure drop in the heat sink decreases, whereas thermal resistance increases since the effective resistance for the flow decreases. Note that for $CL_s=0$ and $CL_t=0$, the entire flow goes through the heat sink and the total thermal resistance of the heat sink is minimum. Thus, the thermal resistance is a direct measure of the deterioration of the thermal performance due to the presence of side and top bypass regions around the heat sink. However, with both side and top clearance ratios, the thermal performance increases further. In each case, the optimum point (where R_{th} and ΔP intersect) increases with the increase in CL_t but remains fixed for CL_s.

The effect of side and top clearances on the dimensionless entropy generation rate is shown in Fig. 3 for fixed pin diameter and volume flow rate. The optimum entropy generation rate remains constant with the increase in side clearance and the decrease in top clearance. It is due to the complex behavior of the entropy generation rate due to the increase/decrease in side/top clearance ratios.

Figure 4 shows the effects of the pin diameter and side clearance ratios on the dimensionless entropy generation rate for an in-line arrangement. It is obvious from the figure that for a fixed top clearance ratio, the dimensionless entropy generation rate decreases with the increase in side clearance ratio and the decrease in pin diameter. In the in-line arrangement, with the decrease in

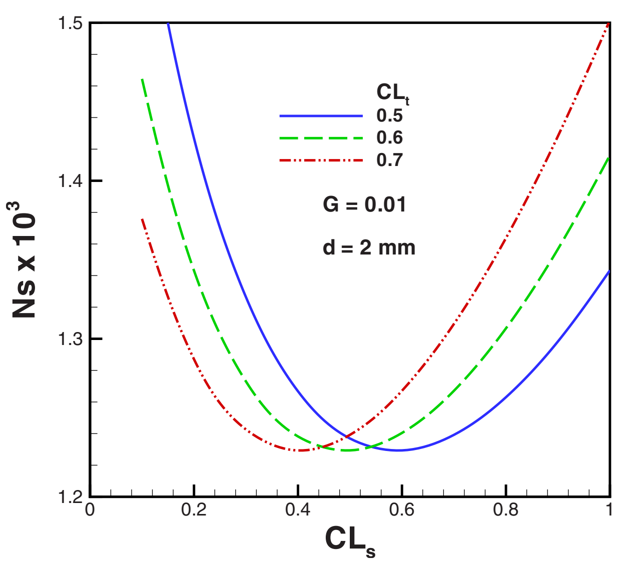

Fig. 3 Dimensionless entropy generation rate versus the side and top clearances

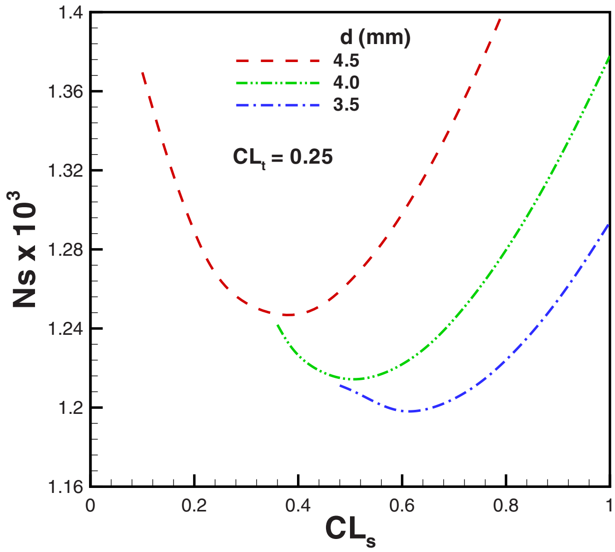

Fig. 4 Dimensionless entropy generation rate versus the side clearance for different pin diameters

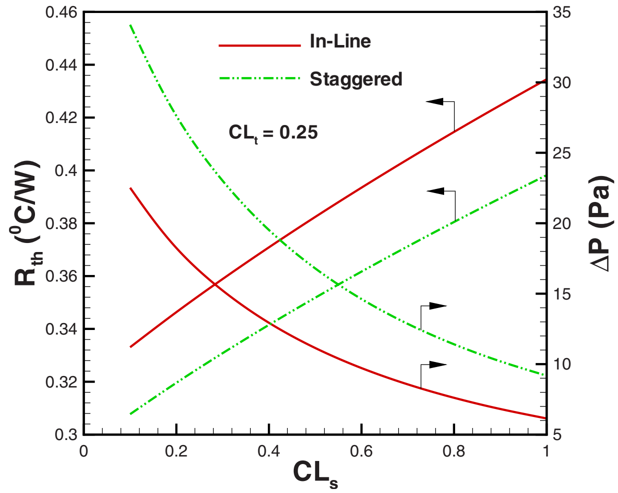

Fig. 6 Comparison of the thermal resistance and the pressure drop for in-line and staggered arrangements

pin diameter, the heat transfer surface area decreases, which allows the increase in pressure drop keeping the longitudinal or transverse pitch ratios fixed.

The effect of the pin height on the dimensionless entropy generation rate is shown in Fig. 5 for an in-line arrangement. For each pin height, the optimum entropy generation rate and the optimum Reynolds number exist, which decrease with the decrease in pin height and the increase in Reynolds number based on the pin diameter and the maximum velocity U_{max} within the pin-fins. It was observed that U_{max} is maximum when the top clearance ratio is zero and decreases with an increase in CL_t.

The effect of the side clearance ratio on the thermal resistance and the total pressure drop in both in-line and staggered arrangements is shown in Fig. 6 for a fixed top clearance ratio. As expected, in both arrangements, the thermal resistance increases and the pressure drop decreases with an increase in the side clearance ratio. For a fully shrouded heat sink (i.e., $CL_s=0$ and $CL_t=0$), the pressure drop is maximum, whereas the thermal resistance is minimum. The pressure drop in the heat sink decreases with an increase in the side clearance ratio since the effective resistance for the flow decreases. The staggered arrangement shows a higher pressure drop in the heat sink and a lower thermal resistance for any CL_s.

The effects of the pin height on the performance of cylindrical pin-fin heat sinks in the side bypass flow are shown in Fig. 7 for both arrangements. The optimum dimensionless entropy generation rate decreases with the decrease in pin heights for both arrangements. The in-line arrangement performs much better for all three cases. The optimum Reynolds number increases with a decrease in pin height for both arrangements. Figure 7 also shows the effects of the Reynolds number on the performance of heat sinks in the side bypass flow for both arrangements. For different pin heights, in-line arrangements give better performance for higher Reynolds numbers and smaller pin heights.

6 Conclusions

An optimal design of cylindrical pin-fin heat sinks in side and top bypass flows is obtained for both the in-line and staggered arrangements. The effects of side and top clearance ratios, pin diameter, pin height, and Reynolds numbers are examined with respect to their roles in influencing optimum design conditions and the overall performance of the pin-fin heat sink. It is demonstrated that

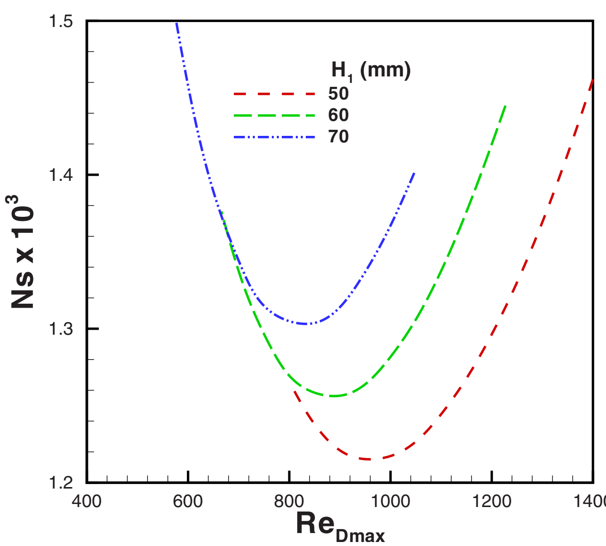

Fig. 5 Dimensionless entropy generation rate versus the side clearance for different pin heights

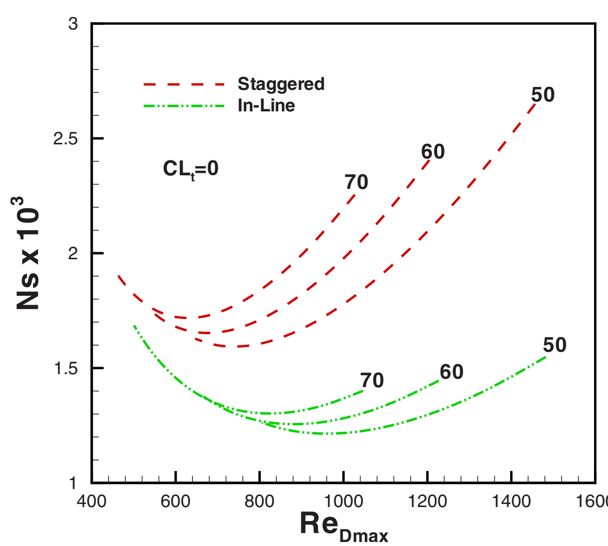

Fig. 7 Comparison of the dimensionless entropy generation rate for in-line and staggered arrangements

1. The thermal resistance increases, whereas the pressure drop decreases with the increase in the side and/or top clearance ratios.
2. The dimensionless entropy generation rate decreases with the increase in the side/top clearance ratio and a decrease in the pin diameter.
3. The optimum dimensionless entropy generation rate and Reynolds numbers decrease with the decrease in pin height.
4. The staggered arrangement shows a higher pressure drop and a lower thermal resistance for any clearance ratio.
5. The in-line arrangement shows better performance for any pin height and side/top clearance ratio.

Acknowledgment

The authors gratefully acknowledge the financial support of Natural Sciences and Engineering Research Council of Canada and the Center for Microelectronics Assembly and Packaging.

Nomenclature

A_b = area of the baseplate $\equiv L\times W_2$, m^2
A_f = frontal face area of the heat sink, m^2
a = dimensionless longitudinal pitch $\equiv S_L/D$
b = dimensionless transverse pitch $\equiv S_T/D$
c = dimensionless diagonal pitch $\equiv S_D/D$
C_1, C_2 = constants defined in Eq. (3)
CL_s = side clearance ratio $\equiv 2W_1/W_2$
CL_t = top clearance ratio $\equiv H_2/H_1$
c = dimensionless diagonal pitch $\equiv S_D/D$
D = pin diameter, m
D_h = hydraulic diameter, m
f = friction factor
g, l = equality and inequality constraints
G = volume flow rate, m^3/s
H = height of the duct, m
h = average heat transfer coefficient, W/m^2 K
j = number of imposed constraints
K_c = correction factor defined in Eq. (23)
K_1, K_2, K_3 = constants defined in Eq. (5)
k = thermal conductivity, W/m K
k_c, k_e = contraction and expansion coefficients in the heat sink region
$\mathcal{L}$ = Lagrangian function
L = length of heat sink in the flow direction, m
$\dot{m}$ = mass flow rate, kg/s
m = fin performance parameter defined in Eq. (16), m^{-1}
N = total number of pins in the heat sink $\equiv N_T N_L$
N_L = number of pins in the longitudinal direction
N_T = number of pins in the transverse direction
Nu_D = Nusselt number based on the pin diameter $\equiv D_h/k_f$
N_s = dimensionless entropy generation rate $\equiv \dot{S}_{\mathrm{gen}}/(Q^2 U_{\max}/k_f \nu T_a^2)$
P = pressure, Pa
Pr = Prandtl number $\equiv \nu/\alpha$
Q = total heat transfer rate, W
R_c = contact resistance between fins and the baseplate, K/W
R_{film} = thermal resistance of exposed (unfinned) surface of the baseplate, K/W
R_{fin} = resistance of a fin, K/W
R_m = material resistance of the baseplate, K/W
Re_D = Reynolds number based on the pin diameter $\equiv DU_{\max}/\nu$
Re_{D_h} = Reynolds number based on the hydraulic diameter $\equiv D_h U/\nu$
S_D = diagonal pitch, m
S_L = longitudinal distance between two consecutive pins, m
S_T = transverse distance between two consecutive pins, m
T = temperature, K
t_b = thickness of the baseplate, m
U = velocity, m/s
U_{app} = approach velocity, m/s
$U_{\max}$ = maximum velocity in the minimum flow area, m/s
W = width of the duct, m
W_2 = width of the heat sink, m

Greek Symbols

ΔP = pressure drop, Pa
η_{fin} = fin efficiency $\equiv \tanh(mH_{\mathrm{fin}})/(mH_{\mathrm{fin}})$
γ = aspect ratio $\equiv H_{\mathrm{fin}}/D$
μ = absolute viscosity of fluid, kg/m s
ν = kinematic viscosity of fluid, m^2/s
ρ = fluid density, kg/m^3

Subscripts

1 = side bypass
2 = top bypass
a = ambient
b = baseplate or unfinned surface of baseplate
d = duct
f = fluid
fin = single fin
fins = all fins with exposed baseplate area
hs = heat sink
m = bulk material
T = thermal
w = wall

References

[1] Lei, N., and Ortega, A., 2004, "Experimental Hydraulic Characterization of Pin Fin Heat Sinks With Top and Side Bypass," *9th Intersociety Conference on Thermal and Thermomechanical Phenomena in Electronic Systems*, Las Vegas, NV, Jun. 1–4, Vol. 1, pp. 418–428.
[2] Urdaneta, M., Ortega, A., and Westphal, R. V., 2003, "Experiments and Modeling of the Hydraulic Resistance of In-Line Square Pin Fin Heat Sinks With Top Bypass Flow," *Advances in Electronic Packaging International Electronic Packaging Technical Conference and Exhibition*, Maui, HI, Jul. 6–11, Vol. 2, pp. 587–596.
[3] Urdaneta, M., and Ortega, A., 2003, "Experiments and Modeling of the Thermal Resistance of In-Line Square Pin-Fin Heat Sinks With Top Bypass Flow," *Advances in Electronic Packaging International Electronic Packaging Technical Conference and Exhibition*, Maui, HI, Jul. 6–11, Vol. 2, pp. 597–604.
[4] Dogruoz, M. B., Urdaneta, M., and Ortega, A., 2002, "Experiments and Modeling of the Heat Transfer of In-Line Square Pin-Fin Heat Sinks With Top Bypass Flow," *American Society of Mechanical Engineers, Heat Transfer Division, ASME International Mechanical Engineering Congress and Exposition*, New Orleans, LA, Nov. 17–22, Vol. 372, pp. 195–206.
[5] Shaukatullah, H., Storr, W. R., Hansen, B. J., and Gaynes, M. A., 1996, "Design and Optimization of Pin Fin Heat Sinks for Low Velocity Applications," IEEE Trans. Compon., Packag. Manuf. Technol., Part A, **19**(4), pp. 486–494.
[6] Rizzi, M., and Catton, I., 2003, "An Experimental Study of Pin Fin Heat Sinks and Determination of End Wall Heat Transfer," *Proceedings of the ASME Summer Heat Transfer Conference*, Las Vegas, NV, Jul. 21–23, Vol. 2003, pp. 445–452.
[7] Rizzi, M., Canino, M., Hu, K., Jones, S., Travkin, V., and Catton, I., 2001, "Experimental Investigation of Pin Fin Heat Sink Effectiveness," *Proceedings of the National Heat Transfer Conference*, Anaheim, CA, Jun. 10–12, Vol. 2, pp. 1235–1243.
[8] Jonsson, H., and Moshfegh, B., 2001, "Modeling of the Thermal and Hydraulic Performance of Plate Fin, Strip Fin, and Pin Fin Heat Sinks—Influence of Flow Bypass," IEEE Trans. Compon. Packag. Technol., **24**(2), pp. 142–149.
[9] Jonsson, H., and Moshfegh, B., 2000, "Modeling of the Thermal and Hydraulic Performance of Plate Fin, Strip Fin, and Pin Fin Heat Sinks—Influence of Flow Bypass," *Seventh Intersociety Conference on Thermal and Thermomechanical Phenomena in Electronic Systems (ITherm 2000)*, Las Vegas, NV, May 23–26, Vol. 1, pp. 185–192.
[10] Jonsson, H., and Moshfegh, B., 2002, "Enhancement of the Cooling Performance of Circular Pin Fin Heat Sinks Under Flow Bypass Conditions, Thermomechanical Phenomena in Electronic Systems," *8th Intersociety Conference on Thermal and Thermomechanical Phenomena in Electronic Systems*,

San Diego, CA, May 30–Jun. 1, pp. 425–432.
[11] Jonsson, H., and Moshfegh, B., 2001, "CFD Modeling of the Cooling Performance of Pin Fin Heat Sinks Under Bypass Flow Conditions," Advances in Electronic Packaging, Pacific Rim/International, Intersociety Electronic Packaging Technical/Business Conference and Exhibition, Kauai, HI, Jul. 8–13, Vol. 1, pp. 393–403.
[12] Chapman, C. L., Lee, S., and Schmidt, B. L., 1994, "Thermal Performance of an Elliptical Pin Fin Heat Sink," *Proceedings of the Tenth IEEE Semiconductor Thermal Measurement and Management Symposium*, San Jose, CA, Feb. 1–3 pp. 24–31.
[13] Bejan, A., 1996, *Entropy Generation Minimization*, CRC, New York.
[14] Bejan, A., 2001, "Thermodynamic Optimization of Geometry in Engineering Flow Systems," Int. J. Exergy, **1**(4), pp. 269–277.
[15] Bejan, A., 1978, "General Criterion for Rating Heat-Exchanger Performance," Int. J. Heat Mass Transfer, **21**, pp. 655–658.
[16] Bejan, A., 1996, "Entropy Generation Minimization: The New Thermodynamics of Finite-Size Devices and Finite-Time Processes," J. Appl. Phys., **79**(3), pp. 1191–1218.
[17] Bejan, A., 2002, "Fundamentals of Exergy Analysis, Entropy Generation Minimization, and the Generation of Flow Architecture," Int. J. Energy Res., **26**, pp. 545–565.
[18] Culham, R. J., and Muzychka, Y. S., 2001, "Optimization of Plate Fin Heat Sinks Using Entropy Generation Minimization," IEEE Trans. Compon. Packag. Technol., **24**(4), pp. 159–165.
[19] Khan, W. A., Yovanovich, M. M., and Culham, J. R., 2006, "Effect of Bypass on Overall Performance of Pin Fin Heat Sinks," *9th AIAA/ASME Joint Thermophysics and Heat Transfer Conference*, Hyatt Regency, San Francisco, CA, Jun. 5–8.
[20] Khan, W. A., Yovanovich, M. M., and Culham, J. R., 2006, "Optimization of Microchannel Heat Sinks Using Entropy Generation Minimization Method," *Semiconductor Thermal Measurement and Management Symposium*, Intercontinental Hotel, Dallas, TX, Mar. 14–16.
[21] Khan, W. A., Culham, J. R., and Yovanovich, M. M., 2006, "Optimal Design of Tube Banks in Crossflow Using Entropy Generation Minimization Method," *44th AIAA Aerospace Sciences Meeting and Exhibit*, Reno, NV, Jan. 9–12.
[22] Khan, W. A., Culham, J. R., and Yovanovich, M. M., 2005, "Optimization of Pin-Fin Heat Sinks Using Entropy Generation Minimization," IEEE Trans. Compon. Packag. Technol., **28**(2), pp. 247–254.
[23] Kern, D. Q., and Kraus, A. D., 1972, *Extended Surface Heat Transfer*, McGraw-Hill, New York.
[24] Sonn, A., and Bar-Cohen, A., 1981, "Optimum Cylindrical Pin-Fin," ASME J. Heat Transfer, **103**, pp. 814–815.
[25] Iyengar, M., and Bar-Cohen, A., 1998, "Least-Material Optimization of Vertical Pin-Fin, Plate-Fin, and Triangular-Fin Heat Sinks in Natural Convective Heat Transfer," *Proceedings of the Intersociety Conference on Thermomechanical Phenomena in Electronic Systems (ITHERM)*, Seattle, WA, May, pp. 295–302.
[26] Iyengar, M., and Bar-Cohen, A., 2002, "Least-Energy Optimization of Forced Convection Plate-Fin Heat Sinks," *Proceedings of the Intersociety Conference on Thermomechanical Phenomena in Electronic Systems (ITHERM)*, San Diego, CA, May, pp. 792–799.
[27] Bar-Cohen, A., and Jelinek, M., 1986, "Optimum Arrays of Longitudinal, Rectangular Fins in Convective Heat Transfer," Heat Transfer Eng., **6**(3), pp. 68–78.
[28] Khan, W. A., 2004, "Modeling of Fluid Flow and Heat Transfer for Optimization of Pin-Fin Heat Sinks," Ph.D. thesis, University of Waterloo, Ontario, Canada.
[29] Žukauskas, A., 1972, "Heat Transfer From Tubes in Crossflow," Adv. Heat Transfer, **8**, pp. 93–160.
[30] Stoecker, W. F., 1989, *Design of Thermal Systems*, McGraw-Hill, New York.